Taylor & Francis
Taylor & Francis Group

Journal of Toxicology and Environmental Health, Part A
Current Issues

ISSN: 1528-7394 (Print) 1087-2620 (Online) Journal homepage: http://www.tandfonline.com/loi/uteh20

Multiwalled carbon nanotube-induced pulmonary inflammatory and fibrotic responses and genomic changes following aspiration exposure in mice: A 1-year postexposure study

Brandi N. Snyder-Talkington, Chunlin Dong, Dale W. Porter, Barbara Ducatman, Michael G. Wolfarth, Michael Andrew, Lori Battelli, Rebecca Raese, Vincent Castranova, Nancy L. Guo & Yong Qian

To cite this article: Brandi N. Snyder-Talkington, Chunlin Dong, Dale W. Porter, Barbara Ducatman, Michael G. Wolfarth, Michael Andrew, Lori Battelli, Rebecca Raese, Vincent Castranova, Nancy L. Guo & Yong Qian (2016) Multiwalled carbon nanotube-induced pulmonary inflammatory and fibrotic responses and genomic changes following aspiration exposure in mice: A 1-year postexposure study, Journal of Toxicology and Environmental Health, Part A, 79:8, 352-366, DOI: 10.1080/15287394.2016.1159635

To link to this article: http://dx.doi.org/10.1080/15287394.2016.1159635

View supplementary material

Published online: 19 Apr 2016.

Submit your article to this journal

Article views: 41

View related articles

View Crossmark data

Full Terms & Conditions of access and use can be found at
http://www.tandfonline.com/action/journalInformation?journalCode=uteh20

Download by: [Stephen B. Thacker CDC Library] **Date:** 10 June 2016, At: 07:21

JOURNAL OF TOXICOLOGY AND ENVIRONMENTAL HEALTH, PART A
2016, VOL. 79, NO. 8, 352–366
http://dx.doi.org/10.1080/15287394.2016.1159635

Taylor & Francis
Taylor & Francis Group

Multiwalled carbon nanotube-induced pulmonary inflammatory and fibrotic responses and genomic changes following aspiration exposure in mice: A 1-year postexposure study

Brandi N. Snyder-Talkington[a], Chunlin Dong[b], Dale W. Porter[a], Barbara Ducatman[c], Michael G. Wolfarth[a], Michael Andrew[a], Lori Battelli[a], Rebecca Raese[b], Vincent Castranova[d], Nancy L. Guo[b], and Yong Qian[a]

[a]Pathology and Physiology Research Branch, Health Effects Laboratory Division, National Institute for Occupational Safety and Health, Morgantown, West Virginia, USA; [b]Mary Babb Randolph Cancer Center, West Virginia University, Morgantown, West Virginia, USA; [c]Department of Pathology, West Virginia University, Morgantown, West Virginia, USA; [d]Department of Pharmaceutical Sciences, School of Pharmacy, West Virginia University, Morgantown, West Virginia, USA

ABSTRACT

Pulmonary exposure to multiwalled carbon nanotubes (MWCNT) induces an inflammatory and rapid fibrotic response, although the long-term signaling mechanisms are unknown. The aim of this study was to examine the effects of 1, 10, 40, or 80 μg MWCNT administered by pharyngeal aspiration on bronchoalveolar lavage (BAL) fluid for polymorphonuclear cell (PMN) infiltration, lactate dehydrogenase (LDH) activity, and lung histopathology for inflammatory and fibrotic responses in mouse lungs 1 mo, 6 mo, and 1 yr postexposure. Further, a 120-μg crocidolite asbestos group was incorporated as a positive control for comparative purposes. Results showed that MWCNT increased BAL fluid LDH activity and PMN infiltration in a dose-dependent manner at all three postexposure times. Asbestos exposure elevated LDH activity at all 3 postexposure times and PMN infiltration at 1 mo and 6 mo postexposure. Pathological changes in the lung, the presence of MWCNT or asbestos, and fibrosis were noted at 40 and 80 μg MWCNT and in asbestos-exposed mice at 1 yr postexposure. To determine potential signaling pathways involved with MWCNT-associated pathological changes in comparison to asbestos, up- and down-regulated gene expression was determined in lung tissue at 1 yr postexposure. Exposure to MWCNT tended to favor those pathways involved in immune responses, specifically T-cell responses, whereas exposure to asbestos tended to favor pathways involved in oxygen species production, electron transport, and cancer. Data indicate that MWCNT are biopersistent in the lung and induce inflammatory and fibrotic pathological alterations similar to those of crocidolite asbestos, but may reach these endpoints by different mechanisms.

ARTICLE HISTORY
Received 24 November 2015
Accepted 25 February 2016

Downloaded by [Stephen B. Thacker CDC Library] at 07:21 10 June 2016

The incorporation of nanoparticles and nanomaterials into manufactured products has immense benefits for industrial sectors, such as energy, health, and transportation, but may result in potential adverse effects of material exposures from workplace activities and during the product life cycle (Castranova et al., 2013; Castranova, 2011; NIOSH, 2009, 2013; Kermanizadeh et al., 2016). Unintentional exposure of workers during material production is of concern to the growing field, and it is necessary to determine the potential acute and chronic effects of such exposures (National Institute for Occupational Safety and Health [NIOSH], 2009). Nanoparticles and nanomaterials possess unique properties as compared to their fine-sized counterparts, and these properties may induce unprecedented mechanisms of toxicity unique to the nanotechnology industry (NIOSH, 2013; Oberdorster et al., 2015).

Multiwalled carbon nanotubes (MWCNT) are nanomaterials consisting of concentric, tubular sheets of graphene with high tensile strength but low aerodynamic diameter, enabling easy aerosolization and potential workplace exposures (Castranova, 2011; Castranova et al., 2013). In vivo, inhalation and aspiration exposure of mice to MWCNT (10, 20, 40, or 80 μg) resulted in inflammation and chronic fibrosis (Mercer et al.,

CONTACT Yong Qian yaq2@cdc.gov Pathology and Physiology Research Branch, Health Effects Laboratory Division, National Institute for Occupational Safety and Health, 1049 Willowdale Rd, Morgantown, WV 26505, USA.

Color versions of one or more of the figures in the article can be found online at www.tandfonline.com/uteh.
Supplemental data for this article can be accessed at Publisher weblink.

© 2016 Taylor & Francis

Downloaded by [Stephen B. Thacker CDC Library] at 07:21 10 June 2016

2011; Porter et al., 2010, 2013; Han et al., 2015), with carcinogenesis after pulmonary or intraperitoneal exposure in some animal models (Sargent et al., 2014; Rittinghausen et al., 2014; Nagai et al., 2011). A fraction of deposited MWCNT persists in the alveolar region and may translocate to the pleural cavity (Mercer et al., 2013a, 2013b; Oberdorster et al., 2015). In vitro, exposures to MWCNT (1.2 μg/mL; 0.024, 0.24, 2.4, and 24 μg/cm^2) resulted in genotoxicity, increases in inflammatory protein markers, and altered gene expression reflective of inflammatory and fibrotic signaling (Pacurari et al., 2012; Snyder-Talkington et al., 2013a, 2013b; Hussain et al., 2014; Siegrist et al., 2014; Han et al., 2015).

A major concern surrounding MWCNT exposure is their strong, fibrous structure akin to amphibole asbestos, a well-known carcinogenic material (Pacurari et al., 2010; Donaldson et al., 2013; IARC, 2012). Several in vivo studies demonstrated that both MWCNT and asbestos induce pulmonary inflammation and fibroblast proliferation in mice up to 2 mo postexposure (Vietti et al., 2013; Kodavanti et al., 2014; Rydman et al., 2015). It is well known that exposure to single-walled carbon nanotubes (SWCNT) induced genotoxicity via reactive oxygen species (ROS) generation in human peripheral lymphocytes (Kim and Yu, 2014). To date, there is a gap between potential genotoxic and gene expression effects of MWCNT and their role in associated toxicological pathways, and it remains to be seen whether MWCNT exert similar chronic effects as noted with asbestos. While long-term pulmonary in vivo studies on the influence of SWCNT have been conducted in comparison to asbestos (Shvedova et al., 2014; Teeguarden et al., 2011), the chronic effects of MWCNT exposure in mice in comparison to asbestos have not been examined. The aim of this study was to determine the influence of 1, 10, 40, or 80 μg MWCNT or 120 μg crocidolite asbestos by pharyngeal aspiration on bronchoalveolar lavage (BAL) fluid for polymorphonuclear cell (PMN) infiltration, lactate dehydrogenase (LDH) activity and lung histopathology for inflammatory and fibrotic responses in mouse lungs after 1 yr postexposure. Gene expression changes were measured in mouse lung tissue with increasing doses of MWCNT at 1 yr postexposure to examine potential underlying mechanisms of fibrotic signaling after exposure to MWCNT.

Methods

MWCNT and Crocidolite Asbestos

MWCNT used in this study were obtained from Hodogaya Chemical Company (MWNT-7, lot 05072001K28) and manufactured using a floating reactant catalytic chemical vapor deposition method followed by high-temperature thermal treatment in argon at 2500°C using a continuous furnace (Kim et al. 2005). Extensive characterization of the MWCNT was previously published (Porter et al., 2010). In summary, the number of walls ranged from 20 to 50, median length was 3.86 ± 1.9 μm, and count mean width was 49 ± 13.4 nm. Trace metal contamination was 0.78%, with sodium (Na, 0.41%) and iron (Fe, 0.32%) being the two major metal contaminants. The crocidolite asbestos [$(Na_2(Fe^{III})_2(Fe^{II})_3Si_8O_{22}(OH_2)$] used is this study was originally obtained from a mine in the Kalahari Desert, South Africa (Cheng et al., 1999), and previously characterized. Briefly, asbestos had a median fiber length of 11.5 μm (range: 2–30 μm), diameter of 160–800 nm, surface area of 17.1 m^2/g, and Fe content (% weight) of 18% (Cheng et al., 1999; Shvedova et al., 2014). Endotoxin levels in the MWCNT and asbestos samples were below the levels of detection (Cheng et al., 1999; Porter et al., 2010).

Animals

Male C57BL/J6 mice (7 wk old, weighing 21.19 ± 0.06 g) were obtained from Jackson Laboratories (Bar Harbor, ME). Individual mice were housed 1 per cage in polycarbonate isolator ventilated cages and provided HEPA-filtered air with fluorescent lighting from 0700 to 1900 h. Autoclaved Alpha-Dri virgin cellulose chips and hardwood Beta-chips were used as bedding. Mice were monitored to be free of adventitous viral pathogens, parasites, mycoplasms, *Helicobacter*, and CAR *Bacillus*. Mice were maintained on Harlan Teklad Rodent Diet 7913 (Indianapolis, IN), and tap water was provided ad libitum. Animals were allowed to acclimate for at least 5 d before use. All animals in this

Downloaded by [Stephen B. Thacker CDC Library] at 07:21 10 June 2016

study were housed in an AAALAC-accredited, specific-pathogen-free, and environmentally controlled facility. All animal studies and procedures were approved by the National Institute for Occupational Safety and Health (NIOSH) Animal Care and Use Committee (ACUC).

This study consisted of three components: BAL, pulmonary histopathology, and lung tissue mRNA microarray analysis. Each component consisted of 8 mice per exposure group (dispersion media [DM, negative control]; 1, 10, 40, or 80 μg MWCNT; 120 μg crocidolite asbestos [positive control]) to be sacrificed at 1, 6, or 12 mo post-exposure, for a total of 144 mice per each arm of BAL, pulmonary histopathology, and lung tissue mRNA microarray analysis and 432 mice for the total study.

MWCNT and Crocidolite Asbestos Pharyngeal Aspiration Exposure

A stock suspension of MWCNT (1.6 mg/ml) was prepared in DM (Ca^{2+} and Mg^{2+}-free phosphate-buffered saline, pH 7.4, supplemented with 5.5 m*M* d-glucose, 0.6 mg/mL mouse serum albumin, and 0.01 mg/ml 1,2-dipalmitoyl-sn-glycero-3-phosphocholine) with sonication as previously described by Porter et al. (2008, 2010). Serial dilutions of MWCNT suspension were made using DM as the diluent. Crocidolite asbestos (2.4 mg/ml) was suspended in DM by brief vortexing. Mice were anesthetized with isoflurane (Abbott Laboratories, North Chicago, IL). When fully anesthetized, the mouse was positioned with its back against a slant board and suspended by the incisor teeth using a rubber band. The mouth was opened, and the tongue gently pulled aside from the oral cavity. A 50-μl aliquot of sample was pipetted at the base of the tongue, and the tongue was restrained until at least 2 deep breaths were completed (but for not longer than 15 s). Following release of the tongue, the mouse was lifted off the board, placed on its left side, and monitored for recovery from anesthesia. Mice received either DM; 1, 10, 40, or 80 μg MWCNT; or 120 μg asbestos. Previous comparative studies by our group demonstrated that well-dispersed suspensions of MWCNT given by aspiration exposure result in lung distribution patterns similar to those from MWCNT administered by inhalation exposure, and there is similar structure between MWCNT prepared for aspiration and those prepared for inhalation (Mercer et al., 2010; 2013a; Porter et al., 2010, 2013). An asbestos dose of 120 μg was used in previous studies by our group as a high asbestos dose to compensate for higher fiber counts/mass of SWCNT versus asbestos (Shvedova, 2014). Inflammatory and fibrotic responses to SWCNT and MWCNT are linearly dependent upon dose (Shvedova et al., 2014; Mercer et al., 2011, 2013a).

Bronchoalveolar Lavage

At 1, 6, and 12 mo postexposure, mice were euthanized with pentobarbital (>100 mg/kg body weight, i.p.). A tracheal cannula was inserted and bronchoalveolar lavage (BAL) was performed through the cannula using ice-cold Ca^{2+}- and Mg^{2+}-free phosphate-buffered saline, pH 7.4, supplemented with 5.5 m*M* D-glucose (PBS). The first lavage (0.6 ml) was kept separate from the rest of the lavage fluid. Subsequent lavages, each with 1 ml PBS, were performed until a total of 4 ml lavage fluid was collected. BAL cells were isolated by centrifugation (650 × g, 5 min, 4°C). An aliquot of the acellular supernatant from the first BAL (BAL fluid) was decanted and transferred to tubes for analysis of lactate dehydrogenase (LDH) activity. The acellular supernatants from the remaining lavage samples were decanted and discarded. BAL cells isolated from the first and subsequent lavages of the same mouse were pooled after suspension in PBS, centrifuged a second time (650 × g, 5 min, 4°C), and the supernatant was decanted and discarded. The BAL cell pellet was then suspended in PBS and placed on ice. Total BAL cell counts were obtained using a Coulter Multisizer 3 (Coulter Electronics, Hialeah, FL) and cytospin preparations of the BAL cells were made using a cytocentrifuge (Shandon Elliot Cytocentrifuge, London, UK). The cytospin preparations were stained with modified Wright–Giemsa stain and cell differentials (approximately 200 cells per animal) were determined by light microscopy.

BAL fluid LDH activities were evaluated as a marker of cytotoxicity. BAL fluid LDH activities

Downloaded by [Stephen B. Thacker CDC Library] at 07:21 10 June 2016

were determined by monitoring the LDH catalyzed oxidation of lactate to pyruvate coupled with the reduction of NAD^+ at 340 nm using a commercial assay kit (Roche Diagnostics Systems, Montclair, NJ) using a COBAS MIRA Plus instrument (Roche Diagnostic Systems, Montclair, NJ).

Lung Sample Collection

A second group of mice, which were not lavaged, were euthanized for RNA studies. Mice at 12 mo postexposure were euthanized by pentobarbital (>100 mg/kg body weight, ip) and exsanguination. Lungs were removed, placed into tubes containing RNAlater (Ambion, Austin, TX), and frozen at –80°C.

Lung Histopathology and Pathology

The third group of mice, which were not lavaged or used for RNA studies, was used for histopathology. At 1, 6, or 12 mo postexposure, mice were euthanized with pentobarbital (>100 mg/kg body weight, ip), and euthanasia was completed by exsanguination. Following euthanasia, the lungs were removed and fixed by airway inflation with 1 ml 10% neutral buffered formalin. Lungs were trimmed, processed, and embedded in paraffin. Sections from the left lung lobe were stained with hematoxylin and eosin (H&E) for routine pathology evaluation. In addition, sections of the left lung lobe were stained with Masson's trichrome and Sirius red to evaluate fibrosis. H&E-stained slides were scored for pigmented macrophages, the presence of MWCNT or asbestos, and type and degree of inflammation on a 5-point scale: none (0+), minimal (1+), mild (2+), moderate (3+), marked (4+), using both degree and extent. Fibrosis was evaluated using the same grading scheme, but further included the review of trichrome and Sirius red stains for collagen. Negative and positive control slides were scored using the same system. Fibrosis is either fibroblastic proliferation or collagen deposition in the interstitium of the lung. The degree is based upon quantity of proliferation or deposition present and may be graded based upon widening of the alveolar septae. Minimal would involve very minimal deposition and almost imperceptible widening, mild would be clearly evident as increased interstitial thickness, moderate would start to show some definite remodeling, and severe or marked would involve a pattern with considerable thickening and a honeycomb pattern.

Statistical Analyses

For the BAL studies, comparisons of dose groups at each postexposure time and across time course at each dose were performed using analysis of variance (ANOVA) assuming an unequal variance structure. This was performed using PROC MIXED in statistical analysis system (SAS) 9.3 (Littell et al., 2002). Dose-response significance for MWCNT doses from 0 to 80 μg was determined by examining the p value for main effect for dose, and pairwise comparisons of interest were performed between groups for dose or time course as indicated using variance estimates from the ANOVA. All tests of significance were two-tailed and performed using significance level .05. For the assessment of MWCNT-induced inflammation and fibrosis scores, ANOVA was used to compare the treatment and control groups at statistical significance level of $\alpha = .05$.

Tissue mRNA Extraction

Total RNA was isolated from mouse lung tissue using a *mir*Vana miRNA Isolation Kit from Ambion per the manufacturer's protocol. Mouse lungs were initially disrupted by transferring them to a 2-ml microcentrifuge tube containing 400 μl silica beads and 600 μl Lysis/Binding Solution. Tubes were shaken in a BeadBeater homogenizer for 1.5 min to ensure complete tissue disruption. Following disruption, samples were centrifuged at 10,000 × g (2000 rpm), 4°C, for 10 min to pellet the beads and any undisrupted tissue. Tissue lysates were transferred to new 2-ml tubes, 60 μl miRNA Homogenate Additive was added, and samples were incubated on ice for 10 min. One volume (600 μl) of acid-phenol:chloroform was added, and the lysate was vortexed for 60 s, followed by centrifugation at 10,000 × g (2000 rpm), 4°C, for 5 min. The aqueous (upper) layer was removed and transferred to a new microcentrifuge tube, followed by the addition of 1.25 vol of room-temperature 100% ethanol. The lysate was mixed thoroughly and passed through a

filter cartridge by centrifugation at 10,000 × g (2000 rpm) for 30 sec. Flow-through was discarded, and the filter was washed once with wash buffer 1, twice with 500 µl wash buffer 2/3, and total RNA was eluted using 100 µl 95°C RNase-free water. RNA concentrations were determined using a NanoDrop 1000 Spectrophotometer (NanoDrop Technologies, Wilmington, DE), and RNA quality was assessed using an Agilent 2100 Bioanalyzer (Agilent Technologies, Santa Clara, CA).

mRNA Microarray Processing

The mRNA microarray consisted of 41,345 probes. Variance was calculated for each probe across all samples to remove any probe with variance >0.2. All probes resulted in variance <0.2; therefore, no probes were removed due to variance. Unknowns were then removed from the data, leaving 25,616 probes. Data analysis was performed with 26,191 probes. ANOVA was used to compare each treatment group at each postexposure time point to its respective DM control to determine significantly up- and downregulated mRNA with a p value <.05, false discovery rate (FDR) of 10%, and fold change (FC) ≥1.5 (Supplemental File 1).

Ingenuity Pathways Analysis (IPA)

Data were analyzed and networks and functional analyses were generated through the use of QIAGEN's Ingenuity Pathways Analysis (IPA®, QIAGEN, Redwood City, CA, www.qiagen.com/ingenuity). IPA was used to determine associations of changes in mRNA with canonical pathways and diseases and functions. Molecules are represented as nodes, and the biological relationship between two nodes is represented as an edge (line). All edges are supported by at least one reference from the literature, from a textbook, or from canonical information stored in the Ingenuity Knowledge Base. Human, mouse, and rat orthologs of a gene are stored as separate objects in the Ingenuity Knowledge Base but are represented as a single node in the network. Nodes are displayed using various shapes that represent the functional class of the gene product.

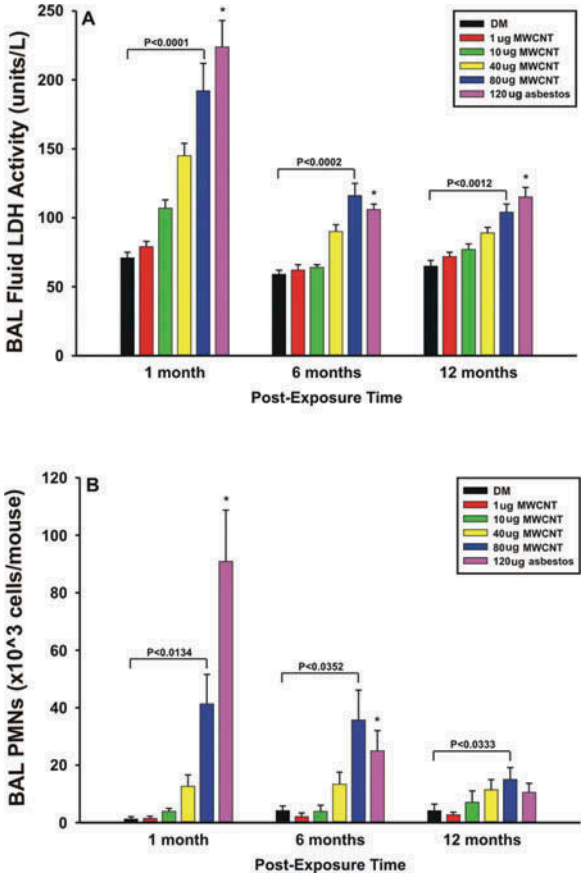

Figure 1. Bronchioalveolar lavage fluid (BAL) lactate dehydrogenase (LDH) activity and polymorphonuclear lymphocytes (PMN). Mice were exposed by pharyngeal aspiration to dispersion medium (DM: vehicle), MWCNT (1, 10, 40, or 80 µg/mouse) or crocidolite asbestos (120 µg/mouse). BAL studies were conducted at 1, 6, and 12 mo postexposure. Values are means ± SE (n = 6–8). Bracket above bars indicates p value for dose-dependent MWCNT effect at each postexposure time. Asterisk indicates asbestos-exposed group was significantly higher in comparison to the corresponding vehicle-exposed group at that postexposure time. Significance was set at $p \leq .05$.

Results

Lactate Dehydrogenase (LDH) Activity and Polymorphonuclear (PMN) Cells

Bronchoalveolar (BAL) fluid LDH activity was determined as an indicator of cytotoxicity (Figure 1A), while polymorphonuclear cells (PMN) infiltration obtained by whole lung lavage was determined as an indicator of pulmonary inflammation (Figure 1B). A significant dose response to MWCNT exposure was observed at all three postexposure time points for both BAL fluid LDH activity and PMN infiltration, with MWCNT-induced damage and inflammation

Downloaded by [Stephen B. Thacker CDC Library] at 07:21 10 June 2016

markedly decreasing with time postexposure. In addition, asbestos-exposed mice displayed significantly higher BAL fluid LDH levels than vehicle-exposed mice at all 3 postexposure times, but PMN values obtained from asbestos-exposed mice were only higher at 1 and 6 mo postexposure.

Lung Histopathology

Each H&E-, trichrome-, or Sirius red-stained lung section was evaluated on a scale of 0–4 (none, minimal, mild, moderate, and marked, respectively). None of the slides demonstrated marked fibrosis; the maximal fibrosis score was 3+ (moderate). An average fibrosis score was determined for each individual tissue at a specific dose and exposure time by averaging the score for each H&E, trichrome, and Sirius red stain at that time point (Figure 2A). The average fibrosis scores at 1 mo postexposure were 0, 0, 0, 0.37, 1.45, and 1.83 for DM, for 1, 10, 40, and 80 μg MWCNT, and for 120 μg asbestos, respectively. The mean fibrosis scores at 6 mo postexposure were 0, 0, 0, 0.87, 1.55, and 2.2 for DM, for 1, 10, 40, and 80 μg MWCNT, and for 120 μg asbestos, respectively. The average fibrosis scores at 12 mo postexposure were 0, 0, 0.04, 0.83, 1.85, and 2.33 for DM, for 1, 10, 40, and 80 μg MWCNT, and for 120 μg asbestos, respectively. There were significant increases in mean fibrosis score over DM for 40 and 80 μg MWCNT and 120 μg asbestos at each postexposure time.

In addition to fibrosis, the level of inflammation was assessed in each tissue at each dose 1, 6, and 12 mo postexposure (Figure 2B). The degree of inflammation was assessed on a scale of 0–4 (including acute [PMN leukocytes], chronic [lymphocytes and plasma cells], and granulomatous [histiocytes and multinucleated giant cells] inflammation). The mean inflammation scores at 1 mo postexposure were 0, 0.16, 0.25, 0.25, 0.75, and 2.25 for DM, for 1, 10, 40, and 80 μg MWCNT, and for 120 μg asbestos, respectively. The average inflammation scores at 6 mo postexposure were 0.125, 0.125, 0.25, 0.62, 0.66, and 2 for DM, for 1, 10, 40, and 80 μg MWCNT, and for 120 μg asbestos, respectively. The mean inflammation scores at 12 mo postexposure were 0, 0.12, 0.12, 0.37, 0.57, and 2 for DM, for 1, 10, 40, and 80 μg MWCNT, and for 120 μg asbestos, respectively. There was significant elevation

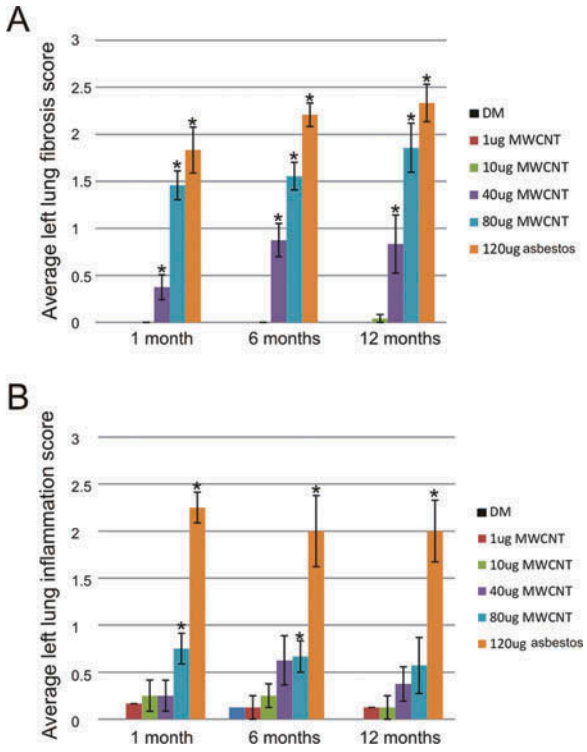

Figure 2. Average left lung fibrosis and inflammation scores. (A) A mean fibrosis score (± standard error) was determined for each individual tissue at each dose and postexposure time by averaging the score for each H&E, trichrome, and Sirius red stain at that time point. Each lung section was evaluated on a 5-point scale: none (0+), minimal (1+), mild (2+), moderate (3+), marked (4+), using both degree and extent; $n = 8$. Asterisk indicates significant change versus DM, $p < .05$. (B) A mean inflammation score (± standard error) was determined for each individual tissue at each dose and postexposure time at that time point. Each lung section was evaluated on a 5-point scale: none (0+), minimal (1+), mild (2+), moderate (3+), marked (4+), using both degree and extent; $n = 8$. Asterisk indicates significant change versus DM, $p < .05$.

in mean inflammation score over DM for 80 μg MWCNT at 1 and 6 mo postexposure and a significant rise in average inflammation score over DM for 120 μg asbestos at all postexposure time points..

At 1 yr postexposure, lungs exposed to DM or 1 or 10 μg MWCNT (Figures 3A3C and Figures 4A4C) were histologically normal. Foreign material was apparent in lungs exposed to 40 and 80 μg MWCNT 1 yr postexposure (Figures 3D, 3E, 4D, and 4E). Pigmented macrophages and mild fibrosis were noted in walls of terminal bronchioles (Figures 3D, 3E, and 4E), fibrosis in alveolar septa (Figures 4D and 4E), and focal tractional emphysema (Figure 4D) after 40 or 80 μg MWCNT exposure. Asbestos exposure induced a foreign body giant cell reaction and fibrosis (Figures 3F and 4F).

Downloaded by [Stephen B. Thacker CDC Library] at 07:21 10 June 2016

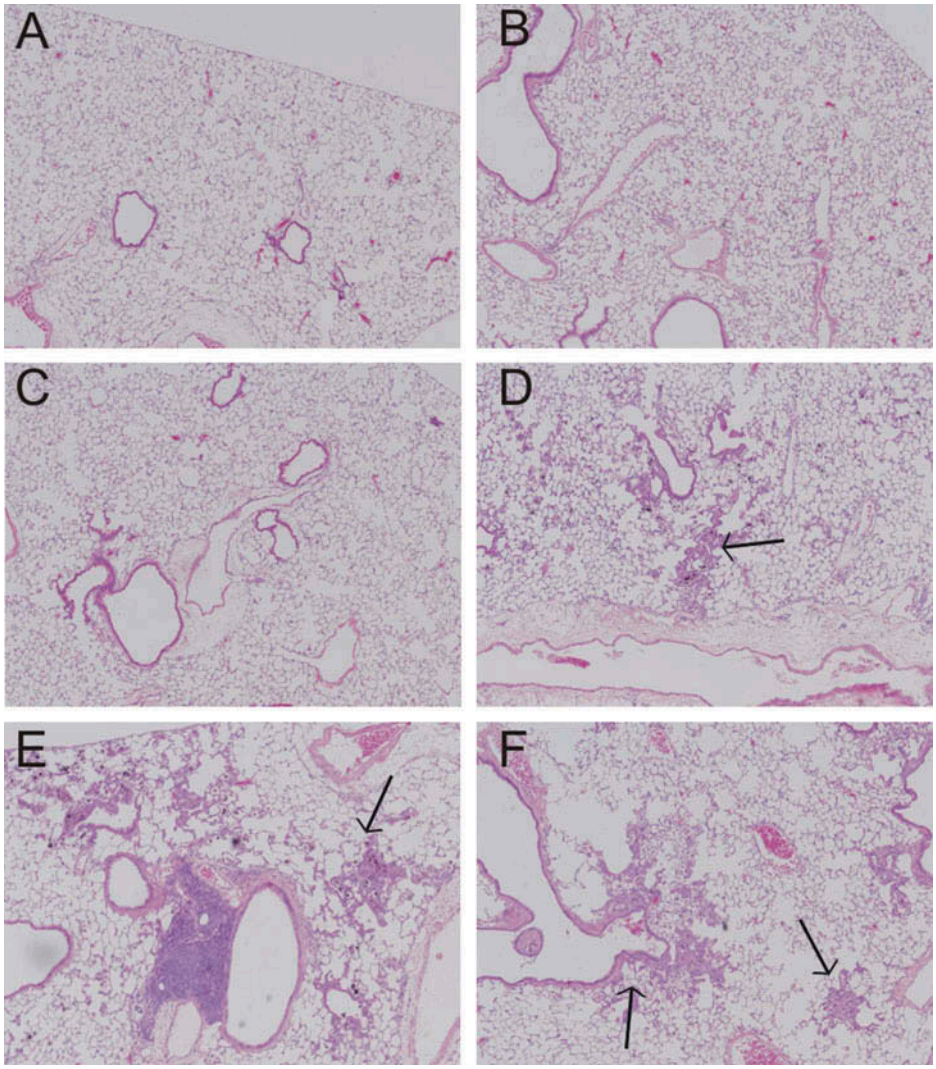

Figure 3. Left lung H&E pathology staining. Lung sections were evaluated for gross pathological changes based upon H&E staining at 4× magnification. Sections from each dose (A: DM, B: 1 μg MWCNT, C: 10 μg MWCNT, D: 40 μg MWCNT, E: 80 μg MWCNT, F: 120 μg asbestos) at 12 mo postexposure are shown. Arrows, where appropriate, indicate the following: (A) unremarkable lung parenchyma with normal alveoli and bronchioles; (B) unremarkable lung parenchyma; (C) no inflammation or fibrosis; (D) fibrotic foci (arrow) in the walls of respiratory bronchioles along with pigmented macrophages; (E) extensive fibrosis in the walls of respiratory bronchioles (arrow); (F) extensive fibrosis around bronchioles and respiratory bronchioles (arrows). Magnification ×4.

Downloaded by [Stephen B. Thacker CDC Library] at 07:21 10 June 2016

Genomic Analysis

Whole lungs were collected from mice exposed by aspiration to DM, to 1, 10, 40, or 80 μg MWCNT, or to 120 μg crocidolite at 12 mo postexposure, processed for mRNA extraction, and analyzed by whole genome microarray. Expression of mRNA at 1, 10, 40, or 80 μg MWCNT or 120 μg crocidolite exposures was compared to expression of mRNA in DM control mice to determine mRNAs that were up- or downregulated in each exposure group. In total, 90, 293, 301, 254, and 350 mRNA were significantly up- or downregulated as compared to control at 12 mo postexposure in the 1-, 10-, 40-, or 80-μg MWCNT or 120-μg crocidolite exposure groups, respectively (Supplemental File 1).

To determine potential canonical pathways and disease and function pathways involving these significant mRNA, analysis and comparison analysis tools in IPA were used. Each set of significant mRNA (90, 293, 301, 254, and 350 mRNA at 12 mo postexposure in the 1-, 10-, 40-, or 80-μg MWCNT or 120-μg crocidolite exposure groups, respectively) was analyzed using an IPA core analysis to determine the associated biological processes, pathways, and molecular networks, with

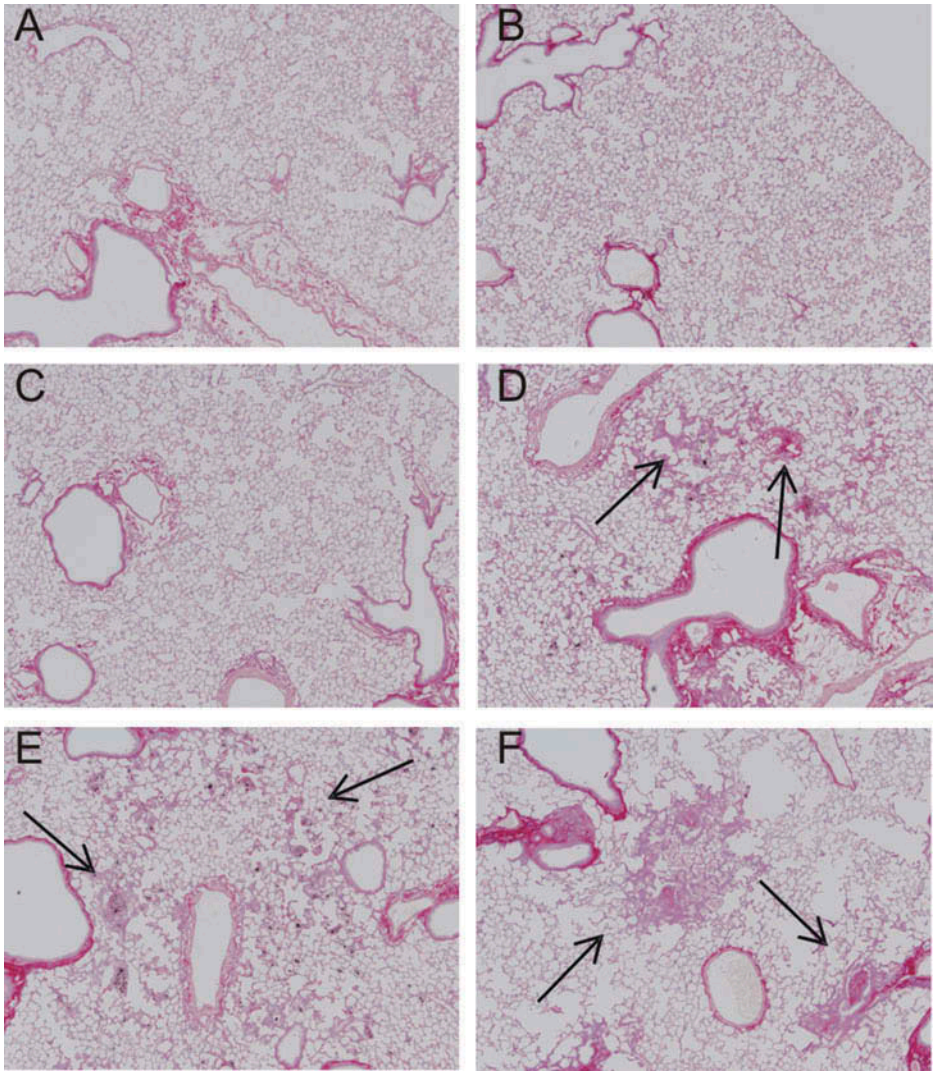

Figure 4. Left lung Sirius red pathology staining. Lung sections were evaluated for visualization of collagen using Sirius red. Sections from each dose (A: DM, B: 1 μg MWCNT, C: 10 μg MWCNT, D: 40 μg MWCNT, E: 80 μg MWCNT, F: 120 μg asbestos) at 12 mo postexposure are shown. Arrows, where appropriate, indicate the following: (A) no significant staining; (B) no significant staining; (C) no significant staining; (D) increased collagen due to fibrosis in the pulmonary parenchyma (arrows) with widening of airspaces due to focal emphysema in association with the traction caused by the scarring; (E) more extensive staining due to increased collagen deposition and fibrosis in the alveolar and bronchiolar walls (arrows); (F) increased fibrosis and collagen deposition (arrows). Magnification ×4.

Downloaded by [Stephen B. Thacker CDC Library] at 07:21 10 June 2016

restricted analysis to only those associations within lung (epithelial, endothelial, fibroblast, and immune) cells and lung tissue. These analyses were then compared to each other to identify changes in biological states across experimental conditions. The top 10 IPA canonical pathways in which exposures to 1, 10, 40, or 80 μg MWCNT or 120 μg asbestos were all associated were Parkinson's signaling, mitochondrial dysfunction, oxidative phosphorylation, hematopoiesis from pluripotent stem cells, protein ubiquitination, CD27 signaling in lymphocytes, communication between innate and adaptive immune cells, T-cell receptor signaling, TCA cycle II (eukaryotic), and primary immunodeficiency signaling (Figure 5). The top 10 IPA diseases and functions in which 1, 10, 40, or 80 μg MWCNT or 120 μg asbestos were all associated were cell-mediated immune response, cellular development, cellular function and maintenance, hematological system development and function, hematopoiesis, cell-to-cell signaling and interaction, cell death and survival, cancer, organ morphology, and tissue development (Figure 6). Because inflammation and fibrosis were endpoints noted by histopathology, the "grow" feature of

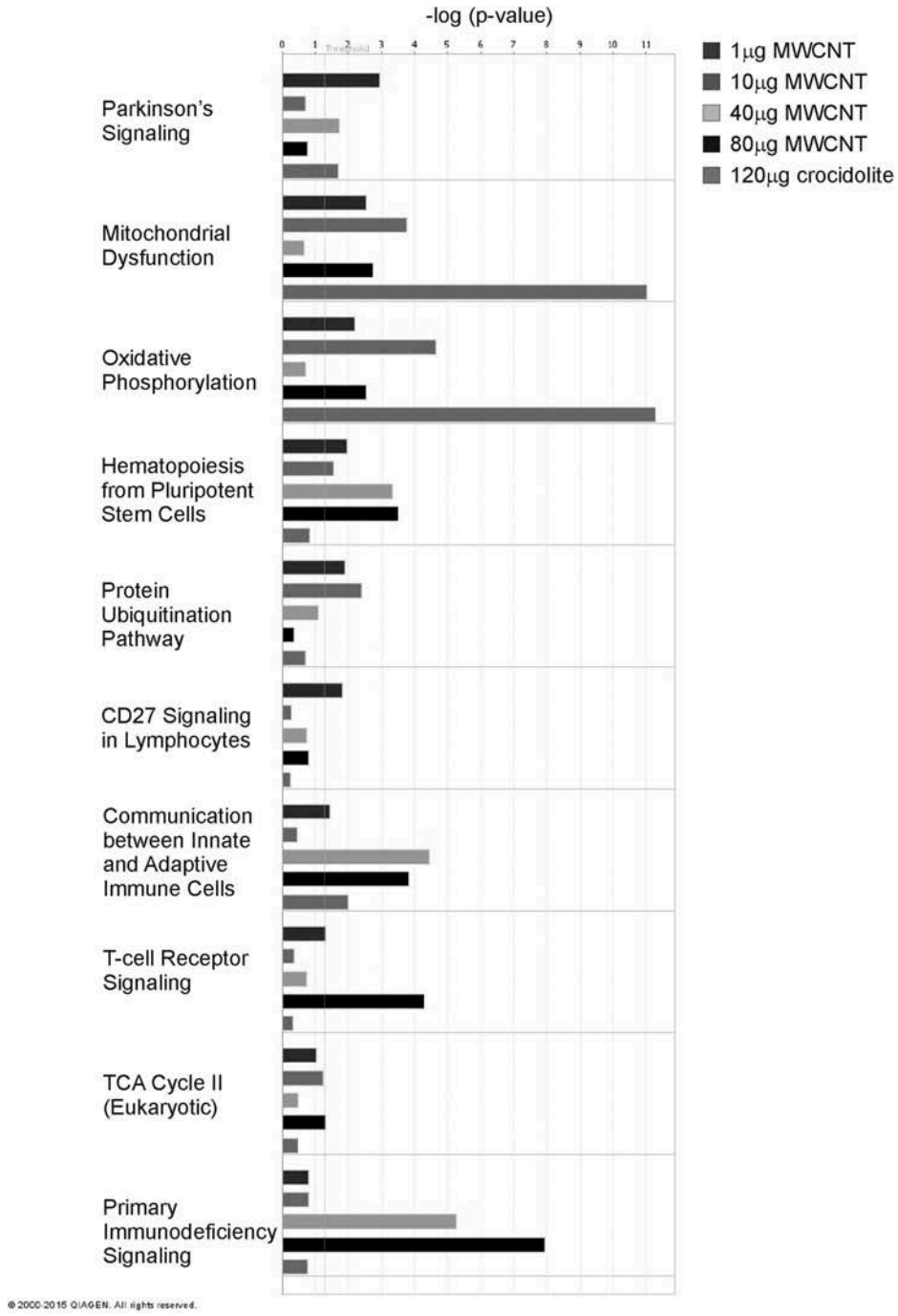

Figure 5. Canonical pathways. The top 10 canonical pathways in lung tissue at 1 yr postexposure in which 1, 10, 40, or 80 μg MWCNT or 120 μg asbestos were associated were determined by IPA analysis and comparison analysis.

IPA, a way to connect a molecule with a disease or function based upon a connection found in the published literature, was employed to identify mRNA changes associated with IPA disease and functions "Inflammatory Response" and "Fibrosis" after 1 yr postexposure (Table 1 and Supplemental Figure 1). MWCNT exposure altered mRNA regulation for many "Inflammatory Response" and "Fibrosis" genes (Table 1).

Discussion

In these studies pharyngeal aspiration was proposed as the method of exposure. The relevance of a bolus exposure to particles, such as that

Downloaded by [Stephen B. Thacker CDC Library] at 07:21 10 June 2016

Downloaded by [Stephen B. Thacker CDC Library] at 07:21 10 June 2016

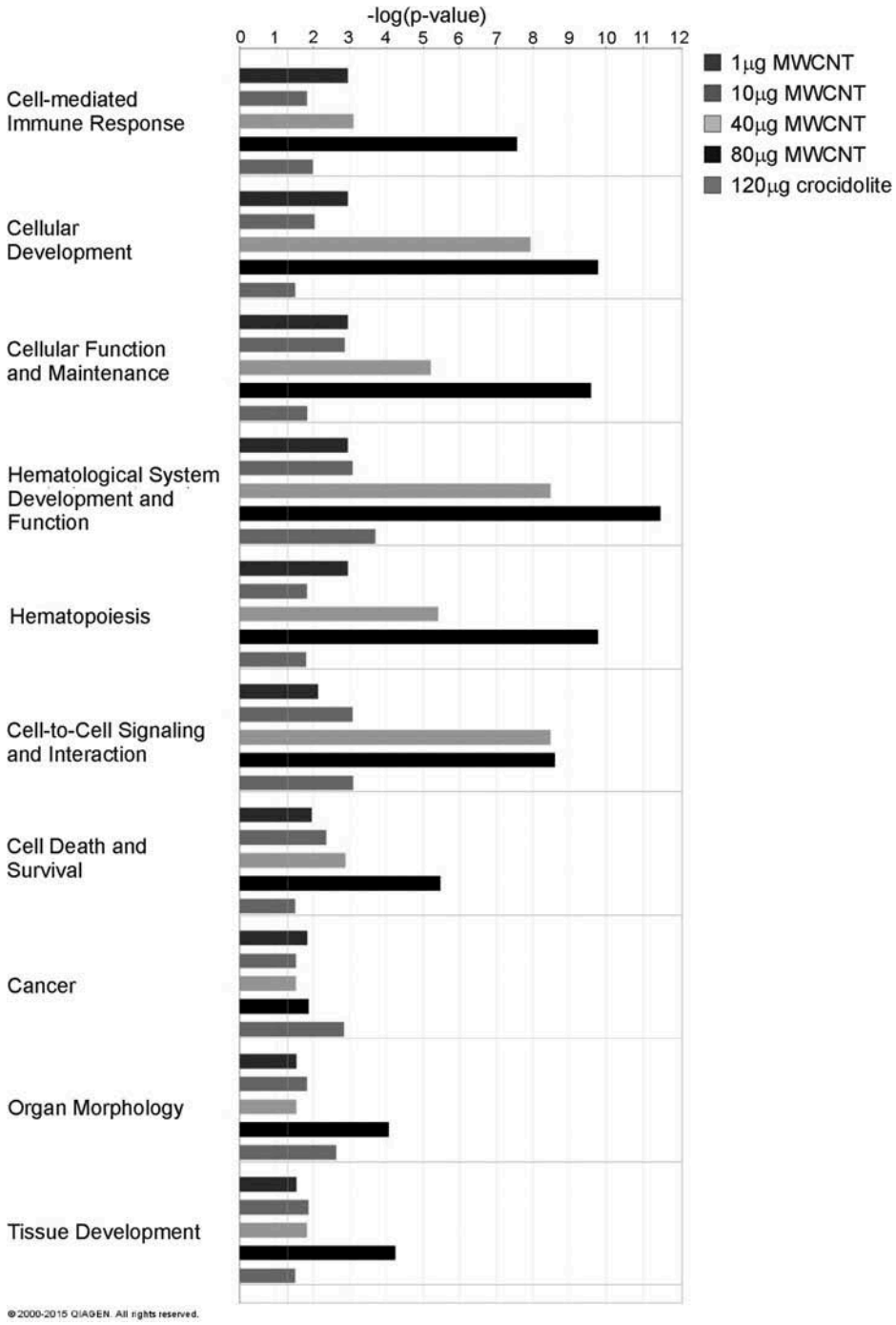

Figure 6. Diseases and functions. The top 10 diseases and functions at 1 yr postexposure in which 1, 10, 40, or 80 μg MWCNT or 120 μg asbestos were associated were determined by IPA analysis and comparison analysis.

delivered by pharyngeal aspiration, to pulmonary responses resulting from inhalation exposure, is a long-standing debate in pulmonary toxicology. The results of two previous studies by our lab, one using pharyngeal aspiration (Porter et al., 2010) and the other using whole body inhalation (Porter et al., 2013), afforded a unique opportunity to address this issue. A comparison of the inflammatory responses 1 d after exposure showed that the degree of infiltration of PMN into the airspaces after pharyngeal aspiration (10 μg MWCNT dose) did not significantly differ from the inflammatory response after inhalation of MWCNT (13 μg MWCNT lung burden) (Porter et al., 2013). Further, lung samples obtained from the MWCNT pharyngeal aspiration study (Porter

Table 1. Up- and downregulated genes in lung tissue involved in Ingenuity Pathways Analysis inflammatory response and fibrosis

	Inflammatory response	Fibrosis
1 μg MWCNT	Upregulated: *alox5ap, mefv, ptger3, ptger1* Downregulated: *park7*	Upregulated: *ptger1*
10 μg MWCNT	Upregulated: *ccl19, ntn1, serpina3, mmp7* Downregulated: *ndfip1, coro1a, park7, tyrobp, plaa, sharpin, parp1, lgals1, ptger4, lsp1, ets1, myd88, ccr2, ighm, nfkb1*	Upregulated: *mmp7* Downregulated: *gstp1, bax, cdk4, ets1, myd88, ccr2, ighm, nfkb1*
40 μg MWCNT	Upregulated: *ptger3, cd14, nt5e, ptger1* Downregulated: *cirbp, cxcr5, capg, rps19, park7, h2-m3, ccr7, aimp1, h2-q7, sharpin, blnk, mina, ccl5, serpinb1, il1r1, ighm*	Upregulated: *nt5e, ptger1* Downregulated: *ighm, il1r1, serpinb1, kcnn4, cd19, gnb2l1*
80 μg MWCNT	Downregulated: *cyba, ccl5, blnk, rps19, ptpn6, cd69, lsp1, zfp36, coro1a, park7, ndfip1, sharpin, tnip1, serpinb1, il1b, ets1, ighm, psen1, il17ra, nfkb1, ikbkb, tp53*	Downregulated: *cd19, ddx5, tnfrsf13b, tgfbr2, serpinb1, il1b, ets1, ighm, psen1, il17ra, nfkb1, ikbkb, tp53*
120 μg asbestos	Upregulated: *ccl19* Downregulated: *ecm1, cyba, ndfip1, gpx4, cst3, ctla2b, rps19, map2k2, trpc6, ccl5, park7, sdc4, mif, il1b, ada, pf4*	Downregulated: *nfe2, gstp1, bax, hbb, mif, il1b, ada, pf4*

Note. Analyzed at 1 yr postexposure following pharyngeal aspiration.

Downloaded by [Stephen B. Thacker CDC Library] at 07:21 10 June 2016

et al., 2010) and whole body inhalation study (Porter et al., 2013) were employed for morphometric analyses of MWCNT distribution. One day after pharyngeal aspiration, 18% of MWCNT structures were in the airways and 81% were in the alveolar region of the lung (Mercer et al., 2010), while after whole body inhalation 16% of MWCNT structures were in the airways and 84% were in the alveolar region (Mercer et al., 2013a). Thus, the distribution of MWCNT in the lungs was similar between the two exposure methods. Finally, MWCNT were found to reach the pleural space after both pharyngeal aspiration and inhalation (Porter et al., 2010; Mercer et al., 2013b). Therefore, pharyngeal aspiration of a well-dispersed suspension of MWCNT appears to result in a pulmonary distribution and inflammatory response that closely simulates whole body inhalation.

In order to evaluate the relevance of data obtained in this mouse study to humans, it was necessary to determine whether the doses used in mice are relevant to human occupational exposures. MWCNT-containing airborne dust levels of approximately 400 μg/m^3 were reported by Han et al. (2008). Given the mouse alveolar epithelium surface area is estimated to be 0.05 m^2 (Stone et al., 1992), using the 10–80 μg MWCNT dose range would result in 200–1600 μg MWCNT/m^2 mouse alveolar epithelium. In our whole body MWCNT inhalation study, data demonstrated that MWCNT mass median aerodynamic diameter (MMAD) was 1.3 μm (Porter et al., 2013). For a person performing light work, if one estimates a minute ventilation of 20 L/min (Galer et al., 1992), deposition fraction of 30% (Phalen, 1984), and human alveolar epithelium surface area of 102 m^2 (Stone et al., 1992), the human exposure per month would be 226 μg MWCNT/m^2 alveolar epithelium. Consequently, in a work environment with a MWCNT aerosol of 400 μg/m^3, the 10 μg MWCNT exposure in mouse approximates human deposition for 1 mo. Even if the average daily MWCNT aerosol is determined to be lower, for example, 4 μg/m^3, the 10 μg MWCNT exposure in mouse thus approximates human deposition for an individual performing light work for approximately 7.5 yr. Data suggest that MWCNT doses used in this study approximate reasonable human occupational exposures to MWCNT.

BAL fluid LDH activity was evaluated as a direct measure of lung tissue cytotoxicity. LDH, a cytoplasmic enzyme, is released extracellularly due to cellular damage or death and is used as a marker in BAL fluid to indicate the extent of cytotoxicity in response to a respirable toxicant (Drent et al., 1996; Sager et al., 2013). BAL fluid LDH activity increased significantly in a dose-dependent manner at each 1-, 6-, and 12-mo MWCNT postexposure period, although there was a time-dependent decrease in overall LDH activity after 1 mo for mice exposed to 10, 40, or 80 μg MWCNT that remained relatively unchanged between 6 and 12 mo postexposure. At each postexposure time point, BAL fluid LDH activity in asbestos-exposed mice was significantly higher than for the vehicle control, with a similar time-dependent fall after 1 mo postexposure. In addition, BAL PMN infiltration was evaluated as a

Downloaded by [Stephen B. Thacker CDC Library] at 07:21 10 June 2016

measure of pulmonary inflammation. During pulmonary insult and the ensuing inflammatory response, PMN degranulate, releasing a number of cytotoxic molecules that contribute to lung injury (Engels and van Oeveren, 2015). Following MWCNT exposure, PMN infiltration rose in a dose-dependent manner at all postexposure time points. Although PMN levels were lowest following MWCNT exposure at 12 mo postexposure, there was still a significant dose-dependent increase. It is of interest that Sager et al. (2013) also noted that double-walled carbon nanotubes initiated pulmonary inflammation and cytotoxicity as evidenced by elevation in LDH activity and PMN infiltration in mouse lung. PMN levels were significantly higher than control following asbestos exposure at 1 and 6 mo postexposure, but not at 1 yr. Strong fibers that resist damage or modification after exposure are known to be biopersistent (Donaldson et al., 2013). The MWCNT used in this study, as well as amphibole asbestos, are known for their biopersistence and potential to induce lung injury long after an initial exposure (Donaldson et al., 2013; Donaldson and Seaton, 2012; Mercer et al., 2013a; Wylie and Candela, 2015). Biopersistence, cytotoxicity, and chronic inflammation play critical roles in the development of asbestosis and neoplasia following asbestos exposure (Donaldson et al., 2010; Oberdorster, 2010; Roggli et al., 2010; Stanton et al., 1981). These results indicate that both MWCNT and asbestos have the ability to induce cytotoxicity and an inflammatory response, potentially due to the high aspect ratio and biopersistence of the particles.

While the endpoint for both MWCNT and asbestos exposure may be fibrosis, the mechanisms underlying the development of fibrosis are unknown, and it is possible that MWCNT and asbestos reach this point through different cellular signaling pathways. As the highest levels of fibrosis were seen at 12 mo postexposure, cellular signaling pathways were determined in mouse lung tissue at this time point to determine similarities and differences in signaling pathways between MWCNT and asbestos exposures. Aside from those mice exposed to 1 μg MWCNT, the total number of differentially expressed genes in mice exposed to MWCNT and asbestos were similar (Supplemental File 1). Each set of differentially expressed genes was analyzed using an IPA core analysis, and all resulting core analyses were compared using an IPA comparison analysis to determine the top associated IPA canonical pathways and diseases and functions. In the top 10 IPA canonical pathways to involve genes from each MWCNT and asbestos exposure (Figure 5), the pathways that tended to favor more association with lower exposures to MWCNT were Parkinson's signaling, protein ubiquitination pathways, and CD27 signaling in lymphocytes, which include signaling involved in protein ubiquitination and cell proliferation and survival. Those pathways that tended to favor an association with higher exposures to MWCNT were hematopoiesis from pluripotent stem cells, communication between innate and adaptive immune cells, T-cell receptor signaling, TCA cycle II (eukaryotic), and primary immunodeficiency signaling. These pathways are primarily involved in the immune response, suggesting that higher levels of MWCNT might elicit an immune response up to 1 yr postexposure, particularly immune responses mediated by T cells. Those pathways that tended to favor an association with asbestos included mitochondrial dysfunction and oxidative phosphorylation, both of which are involved in the production of reactive oxygen species (ROS) and electron transport.

In the top 10 IPA diseases and functions to involve genes from each MWCNT and asbestos (Figure 6), there were no apparent diseases and functions that tended to favor an association with lower concentrations of MWCNT than any other exposure. The only disease and function in which asbestos exposure favored an association over MWCNT was cancer. All other top 10 diseases and functions favored higher levels of MWCNT and predominantly involved a response from T lymphocytes and natural killer (NK) cells, along with cellular survival. On the basis of gene expression, it appears that although the same pathological endpoint may be attained, MWCNT and asbestos may induce cellular signaling through differential gene expression, canonical pathways, and functions at the exposure doses applied in this study. Exposure to MWCNT tended to favor those pathways involved in immune responses, specifically T-cell responses, whereas treatment with asbestos tended to favor pathways involved in ROS production, electron transport, and cancer.

Downloaded by [Stephen B. Thacker CDC Library] at 07:21 10 June 2016

As the two common pathological outcomes of MWCNT exposure are pulmonary inflammation and fibrosis, it is conceivable those up- or downregulated genes at 1 yr postexposure were associated with increasing doses of MWCNT that are involved in IPA disease overlays "inflammatory response" or "fibrosis." One gene, *park7*, was downregulated following all MWCNT exposures. Considered to play a protective role against oxidative stress and cell death, the loss of *park7* may indicate a role for this gene following MWCNT administration in oxidative stress and mitochondrial dysfunction (Richarme et al., 2015; Clements et al., 2006). The genes involved in the IPA "inflammatory response" and "fibrosis" disease overlays at increasing doses of MWCNT were associated by IPA with canonical pathways involving oxidative stress and mitochondrial dysfunction at lower concentrations (1 and 10 μg), while higher levels (40 and 80 μg) were correlated with canonical pathways involving interleukin and B- and T-cell signaling. It is potentially through these types of signaling mechanisms that MWCNT may induce their inflammatory and fibrotic responses in lung.

Data demonstrated that MWCNT have the ability to induce inflammation and fibrosis up to 1 yr postexposure. Even though MWCNT are often compared to asbestos in structure and considered to exert similar effects in the lung (Rydman et al., 2015; Vietti et al., 2013), to our knowledge, this is the first long-term exposure study to also include a positive asbestos control for a direct comparison of inflammation- and fibrosis-inducing potential of MWCNT. Lung pathological analysis indicates that asbestos-induced fibrosis is associated with high levels of persistent inflammation, while this disease manifestation does not appear to be correlated with MWCNT-induced fibrosis. With regard to gene expression, increasing doses of MWCNT resulted in aberrant gene expression involving an association with numerous diseases and canonical pathways, particularly those involved in immune responses, which suggests potential cellular and molecular mechanisms involved in MWCNT-induced fibrogenic responses.

Acknowledgments

NLG is supported by the West Virginia Clinical and Translational Science Institute, National Institute of General Medical Sciences, U54GM104942. The findings and conclusions in this report are those of the authors and do not necessarily represent the views of the National Institutes of Health of the National Institute for Occupational Safety and Health. Mention of a brand name does not constitute product endorsement.

References

Castranova, V. 2011. Overview of current toxicological knowledge of engineered nanoparticles. *J. Occup. Environ. Med.* 53: S14–S17.

Castranova, V., Schulte, P. A., and Zumwalde, R. D. 2013. Occupational nanosafety considerations for carbon nanotubes and carbon nanofibers. *Acc. Chem. Res.* 46: 642–649.

Cheng, N., Shi, X., Ye, J., Castranova, V., Chen, F., Leonard, S. S., Vallyathan, V., and Rojanasakul, Y. 1999. Role of transcription factor NF-kappaB in asbestos-induced TNFalpha response from macrophages. *Exp. Mol. Pathol.* 66: 201–210.

Clements, C. M., McNally, R. S., Conti, B. J., Mak, T. W., and Ting, J. P. 2006. DJ-1, a cancer- and Parkinson's disease-associated protein, stabilizes the antioxidant transcriptional master regulator Nrf2. *Proc. Natl. Acad. Sci. USA* 103: 15091–15096.

Donaldson, K., Murphy, F. A., Duffin, R., and Poland, C. A. 2010. Asbestos, carbon nanotubes and the pleural mesothelium: A review of the hypothesis regarding the role of long fibre retention in the parietal pleura, inflammation and mesothelioma. *Part. Fibre Toxicol.* 7: 5.

Donaldson, K., Poland, C. A., Murphy, F. A., Macfarlane, M., Chernova, T., and Schinwald, A. 2013. Pulmonary toxicity of carbon nanotubes and asbestos—Similarities and differences. *Adv. Drug Deliv. Rev.* 65: 2078–2086.

Donaldson, K., and Seaton, A. 2012. A short history of the toxicology of inhaled particles. *Part. Fibre Toxicol.* 9: 13.

Drent, M., Cobben, N. A., Henderson, R. F., Wouters, E. F., and Van Dieijen-Visser, M. 1996. Usefulness of lactate dehydrogenase and its isoenzymes as indicators of lung damage or inflammation. *Eur. Respir. J.* 9: 1736–1742.

Engels, G. E. and Van Oeveren, W. 2015. Biomarkers of lung injury in cardiothoracic surgery. *Dis. Markers* 2015: 472360.

Galer, D. M., Leung, H. W., Sussman, R. G., and Trzos, R. J. 1992. Scientific and practical considerations for the development of occupational exposure limits (OELs) for chemical substances. *Regul. Toxicol. Pharmacol.* 15: 291–306.

Han, J. H., Lee, E. J., Lee, J. H., So, K. P., Lee, Y. H., Bae, G. M., Lee, S. B., Ji, J. H., Cho, M. H., and Yu, I. J. 2008. Monitoring multiwalled carbon nanotube exposure in carbon nanotube research facility. *Inhal Toxicol* 20: 741–749.

Han, S. G., Howatt, D., Daugherty, A., and Gairola, G. 2015. Pulmonary and atherogenic effects of multi-walled carbon nanotubes (MWCNT) in apolipoprotein-E-deficient mice. *J. Toxicol. Environ. Health A*, 78: 244–253.

Hussain, S., Sangtian, S., Anderson, S. M., Snyder, R. J., Marshburn, J. D., Rice, A. B., Bonner, J. C. and Garantziotis, S. 2014. Inflammasome activation in airway

Downloaded by [Stephen B. Thacker CDC Library] at 07:21 10 June 2016

epithelial cells after multi-walled carbon nanotube exposure mediates a profibrotic response in lung fibroblasts. *Part. Fibre Toxicol.* 11: 28.

IARC. 2012. Arsenic, metals, fibres, and dusts. *IARC Monogr. Eval. Carcinogen. Risks Hum.* 100C: 219–296.

Kermanizadeh, A., Gosens, I., MacCalman, L., Johnston, H., Danielsen, P. H., Jacobsen, N. R., Lenz, A.-G., Fernandes, T., Schins, R. P. F., Cassee, F. R., Wallin, H., Kreyling, W., Stoeger, T., Loft, S., Møller, P., Tran, L., and Stone, V. 2016. A multi-laboratory toxicological assessment of a panel of ten engineered nanomaterials to human health—ENPRA project—The highlights, limitations and current and future challenges. *J. Toxicol. Environ. Health B.* 19 *In press*

Kim, Y. A., Hayashi, T., Endo, M., Kaguragi, Y., Tsukada, T., Shan, J., Osato, K., and Tsuruoka, S. 2005. Synthesis and structural characterization of thin multi-walled carbon nanotubes with a partially facetted cross section by a floating reactant method. *Carbon* 43: 2243–2250.

Kim, J. S., and Yu, I. J. 2014. Single-wall carbon nanotubes (SWCNT) induce cytotoxicity and genotoxicity produced by reactive oxygen species (ROS) generation in phytohemagglutinin (PHA)-stimulated male human peripheral blood lymphocytes. *J. Toxicol. Environ. Health A* 77: 1141–1153.

Kodavanti, U. P., Andrews, D., Schladweiler, M. C., Gavett, S. H., Dodd, D. E., and Cyphert, J. M. 2014. Early and delayed effects of naturally occurring asbestos on serum biomarkers of inflammation and metabolism. *J. Toxicol. Environ. Health A*, 77:1024–1039.

Little, R., Stroup, W., and Freund, R. 2002. *SAS for linear models*, 4th ed. SAS Publishing, Cary, North Carolina, USA.

Mercer, R. R., Hubbs, A. F., Scabilloni, J. F., Wang, L., Battelli, L. A., Friend, S., Castranova, V., and Porter, D. W. 2011. Pulmonary fibrotic response to aspiration of multi-walled carbon nanotubes. *Part. Fibre Toxicol.* 8: 21.

Merer, R. R., Hubbs, A. F., Scabilloni, J. F., Wang, L., Battelli, L. A., Schwegler-Berry, D., Castranova, V., and Porter, D. W. 2010. Distribution and persistence of pleural penetrations by multi-walled carbon nanotubes. *Part. Fibre Toxicol.* 7: 28.

Mercer, R. R., Scabilloni, J. F., Hubbs, A. F., Battelli, L. A., McKinney, W., Friend, S., Wolfarth, M. G., Andrew, M., Castranova, V., and Porter, D. W. 2013a. Distribution and fibrotic response following inhalation exposure to multi-walled carbon nanotubes. *Part. Fibre Toxicol.* 10: 33.

Mercer, R. R., Scabilloni, J. F., Hubbs, A. F., A. F., Wang, L., Battelli, L. A., McKinney, W., Castranova, V., and Porter, D. W. 2013b. Extrapulmonary transport of MWCNT following inhalation exposure. *Part. Fibre Toxicol.* 10: 38.

Nagai, H., Okazaki, Y., Chew, S. H., Misawa, N., Yamashita, Y., Akatsuka, S., Ishihara, T., Yamashita, K., Yoshikawa, Y., Yasui, H., Jiang, L., Ohara, H., Takahashi, T., Ichihara, G., Kostarelos, K., Miyata, Y., SHinohara, H., and Toyokuni, S. 2011. Diameter and rigidity of multiwalled carbon nanotubes are critical factors in mesothelial injury and carcinogenesis. *Proc. Natl. Acad. Sci. USA* 108: E1330–E1338.

National Institute for Occupational Safety and Health. 2009. *Approaches to safe nanotechnology: Managing the health and safety concerns associated with engineered nanomaterials.* http://www.cdc.gov/niosh/docs/2010-112c

National Institute for Occupational Safety and Health. 2013. *Protecting the nanotechnology workforce: NIOSH nanotechnology research and guidance strategic plan*, 2013–2016. http://www.cdc.gov/niosh/docs/2014-106

Oberdorster, G. 2010. Safety assessment for nanotechnology and nanomedicine: Concepts of nanotoxicology. *J. Intern. Med.* 267: 89–105.

Oberdorster, G., Castranova V., Asgharian, B., and Sayre, P. 2015. Inhalation exposure to carbon nanotubes (CNT) and carbon nanofibers (CNF): methodology and dosimetry. *J. Toxicol. Environ. Health B* 18: 121–212.

Pacurari, M., Castranova, V., and Vallyathan, V. 2010. Single- and multi-wall carbon nanotubes versus asbestos: Are the carbon nanotubes a new health risk to humans? *J. Toxicol. Environ. Health A* 73: 378–395.

Pacurari, M., Qian, Y., Fu, W., Schwegler-Berry, D., Ding, M., Castranova, V., and Guo, N. L. 2012. Cell permeability, migration, and reactive oxygen species induced by multi-walled carbon nanotubes in human microvascular endothelial cells. *J. Toxicol. Environ. Health A* 75: 129–147.

Phalen, R. F. 1984. Basic morphology and physiology of the respiratory tract. In *Inhalation studies: Foundattions and techniques*, 33–75. Boca Raton, FL: CRC Press.

Porter, D., Sriram, K., Wolfarth, M., Jefferson, A., Schwegler-Berry, D., Andrew, M., and Castranova, V. 2008. A biocompatible medium for nanoparticle dispersion. *Nanotoxicology* 2: 144–154.

Porter, D. W., Hubbs, A. F., Chen, B. T., McKinney, W., Mercer, R. R., Wolfarth, M. G., Battelli, L., Wu, N., Sriram, K., Leonard, S., Andrew, M., Willard, P., Tsuruoka, S., Endo, M., Tsukada, T., Munekane, F., Frazer, D. G., and Castranova, V. 2013. Acute pulmonary dose-responses to inhaled multi-walled carbon nanotubes. *Nanotoxicology* 7: 1179–1194.

Porter, D. W., Hubbs, A. F., Mercer, R. R., Wu, N., Wolfarth, M. G., Sriram, K., Leonard, S., Battelli, L., Schwegler-Berry, D., Friend, S., Andrew, M., Chen, B. T., Tsuruoka, S., Endo, M., and Castranova, V. 2010. Mouse pulmonary dose- and time course-responses induced by exposure to multi-walled carbon nanotubes. *Toxicology* 269: 136–147.

Richarme, G., Mihoub, M., Dairou, J., Bui, L. C., leger, T., and Lamouri, A. 2015. Parkinsonism-associated protein DJ-1/Park7 is a major protein deglycase that repairs methylglyoxal- and glyoxal-glycated cysteine, arginine, and lysine residues. *J. Biol. Chem.* 290: 1885–1897.

Rittinghausen, S., Hackbarth, A., Creutzenberg, O., Ernst, H., Heinrich, U., Leonhardt, A., and Schaudien, D. 2014. The carcinogenic effect of various multi-walled carbon nanotubes (MWCNTs) after intraperitoneal injection in rats. *Part. Fibre Toxicol.* 11: 59.

Roggli, V. L., Gibbs, A. R., Attanoos, R., Churg, A., Popper, H., Cagle, P., Corrin, B., Franks, T. J., Galateau-Salle, F., Galvin, J., Hasleton, P. S., Henderson, D. W., and Honma, K. 2010. Pathology of

asbestosis—An update of the diagnostic criteria: Report of the Asbestosis Committee of the College of American Pathologists and Pulmonary Pathology Society. *Arch. Pathol. Lab. Med*. 134: 462–480.

Rydman, E. M., Ilves, M., Vanhala, E., Vippola, M., Lehto, M., Kinaret, P. A., Pylkkanen, L., Happo, M., Hirvonen, M. R., Greco, D., Savolainen, K., Wolff, H., and Alenius, H. 2015. A single aspiration of rod-like carbon nanotubes induces asbestos-like pulmonary inflammation mediated in part by the IL-1 receptor. *Toxicol Sci*, 147:140–155.

Sager, T. M., Wolfarth, M. W., Battelli, L., Leonard, S. S., Andrew, M., Steinbach, T., Endo, M., Tsuruoka, S., Porter, D. W., and Castranova, V. 2013. Investigation of the pulmonary bioactivity of double-walled carbon nanotubes. *J. Toxicol. Environ. Health A* 76: 922–936.

Sargent, L. M., Porter, D. W., Staska, L. M., Hubbs, A. F., Lowry, D. T., Battelli, L., Siegrist, K. J., Kashon, M. L., Mercer, R. R., Bauer, A. K., Chen, B. T., SAlisbury, J. L., Frazer, D., McKinney, W., Andrew, M., Tsuruoka, S., Endo, M., Fluharty, K. L., Castranova, V., and Reynolds, S. H. 2014. Promotion of lung adenocarcinoma following inhalation exposure to multi-walled carbon nanotubes. *Part. Fibre Toxicol*. 11: 3.

Shvedova, A. A., Yanamala, N., Kisin, E. R., Tkach, A. V., Murray, A. R., Hubbs, A., Chirila, M. M., Keohavong, P., Sycheva, L. P., Kagan, V. E., and castranova, V. 2014. Long-term effects of carbon containing engineered nanomaterials and asbestos in the lung: One year postexposure comparisons. *Am. J. Physiol. Lung Cell Mol. Physiol*. 306: L170–L182.

Siegrist, K. J., Reynolds, S. H., Kashon, M. L., Lowry, D. T., Dong, C., Hubbs, A. F., Young, S. H., Salisbury, J. L., Porter, D. W., Benkovic, S. A., McCawley, M., Keane, M. J., Mastovich, J. T., Bunker, K. L., Cena, L. G., Sparrow, M. C., Sturgeon, J. L., Dinu, C. Z., and Sargent, L. M. 2014. Genotoxicity of multi-walled carbon nanotubes at occupationally relevant doses. *Part. Fibre Toxicol*. 11: 6.

Snyder-Talkington, B. N., Pacurari, M., Dong, C., Leonard, S. S., Schwegler-Berry, D., Castranova, V., Qian, Y., and Guo, N. L. 2013a. Systematic analysis of multiwalled carbon nanotube-induced cellular signaling and gene expression in human small airway epithelial cells. *Toxicol. Sci*. 133: 79–89.

Snyder-Talkington, B. N., Schwegler-Berry, D., Castranova, V., Qian, Y., and Guo, N. L. 2013b. Multi-walled carbon nanotubes induce human microvascular endothelial cellular effects in an alveolar-capillary co-culture with small airway epithelial cells. *Part. Fibre Toxicol*. 10: 35.

Stanton, M. F., Layard, M., Tegeris, A., Miller, E., May, M., Morgan, E., and Smith, A. 1981. Relation of particle dimension to carcinogenicity in amphibole asbestoses and other fibrous minerals. *J. Natl. Cancer Inst*. 67: 965–975.

Stone, K. C., Mercer, R. R., Gehr, P., Stockstill, B., and Crapo, J. D. 1992. Allometric relationships of cell numbers and size in the mammalian lung. *Am. J. Respir. Cell Mol. Biol*. 6: 235–243.

Teeguarden, J. G., Webb-Robertson, B. J., Waters, K. M., Murray, A. R., Kisin, E. R., Varnum, S. M., Jacobs, J. M., Pounds, J. G., Zanger, R. C., and Shvedova, A. A. 2011. Comparative proteomics and pulmonary toxicity of instilled single-walled carbon nanotubes, crocidolite asbestos, and ultrafine carbon black in mice. *Toxicol. Sci*. 120: 123–135.

Vietti, G., Ibouraadaten, S., Palmai-Pallag, M., Yakoub, Y., Bailly, C., Fenoglio, I., Marbaix, E., Lison, D., and Van Den Brule, S. 2013. Towards predicting the lung fibrogenic activity of nanomaterials: Experimental validation of an in vitro fibroblast proliferation assay. *Part. Fibre Toxicol*. 10: 52.

Wylie, A. G., and Candela, P. A. 2015. Methodologies for determining the sources, characteristics, distribution, and abundance of asbestiform and nonasbestiform amphibole and serpentine in ambient air and water. *J. Toxicol. Environ. Health B* 18: 1–42.

Downloaded by [Stephen B. Thacker CDC Library] at 07:21 10 June 2016